

the diameters of the sphere colonies reached a maximum with all of these growth factors together (Fig. 6B). These results suggest that the three growth factors synergistically facilitate the formation and proliferation of the sphere colonies.

*Comparison of the SKPs generated with TGF- $\beta$  with those without TGF- $\beta$*

To examine whether TGF- $\beta$  changes the characteristics of the sphere colonies, the expression of cell surface molecules was assessed by flow cytometry. Although expression profiles of cell surface molecules of the sphere colonies which were generated in the presence of TGF- $\beta$  were almost the same as those of control sphere colonies generated in the absence of TGF- $\beta$  (Fig. 7, middle), the expression of CD71 and CD49f was slightly altered. The mean fluorescence intensity of CD71 and CD49f in the sphere colonies in the absence of TGF- $\beta$  were 0.9 and 0.6. In contrast, the mean fluorescence intensity of CD71 and CD49f in the sphere colonies in the presence of TGF- $\beta$  were 0.5 and 0.8. Analysis showed that there was no difference between the two populations (Fig. 7, top).

Table 1

Quantification of the percentage of differentiation progeny from the sphere colonies under differentiation condition

Antibody	Cell culture conditions for sphere formation	
	EGF+bFGF	EGF+bFGF+TGF $\beta$
$\beta$ III Tubulin	4.2 $\pm$ 1.8%	4.1 $\pm$ 1.2%
GFAP	4.2 $\pm$ 1.7%	3.7 $\pm$ 1.5%
$\alpha$ SMA	4.3 $\pm$ 0.9%	4.3 $\pm$ 0.4%
Oil red O	Highly variable, from 1% to greater than 28%	

Data represent mean  $\pm$  SEM. For differentiation, sphere colonies were trypsinized and dissociated into single cells, and plated at a cell density of 10 cells/ml and in the presence of 1% FBS on the poly-D-lysine/laminin-coated 24-well dishes for 21 days.

Furthermore, to investigate whether the sphere colonies generated in the presence of TGF- $\beta$  were biased to differentiate into certain cell types, the cells from the sphere colonies were cultured in the presence of 1% FBS on poly-D-lysine/laminin-coated 24-well dishes. As shown in Table 1, quantitative analysis of the immunostaining with  $\beta$ III tubulin, GFAP,  $\alpha$ SMA, and staining with Oil red O revealed that cell fate was not affected by TGF- $\beta$ , supporting the hypothesis that the addition of TGF- $\beta$  during the sphere colony formation does not alter the characteristics of the cells.

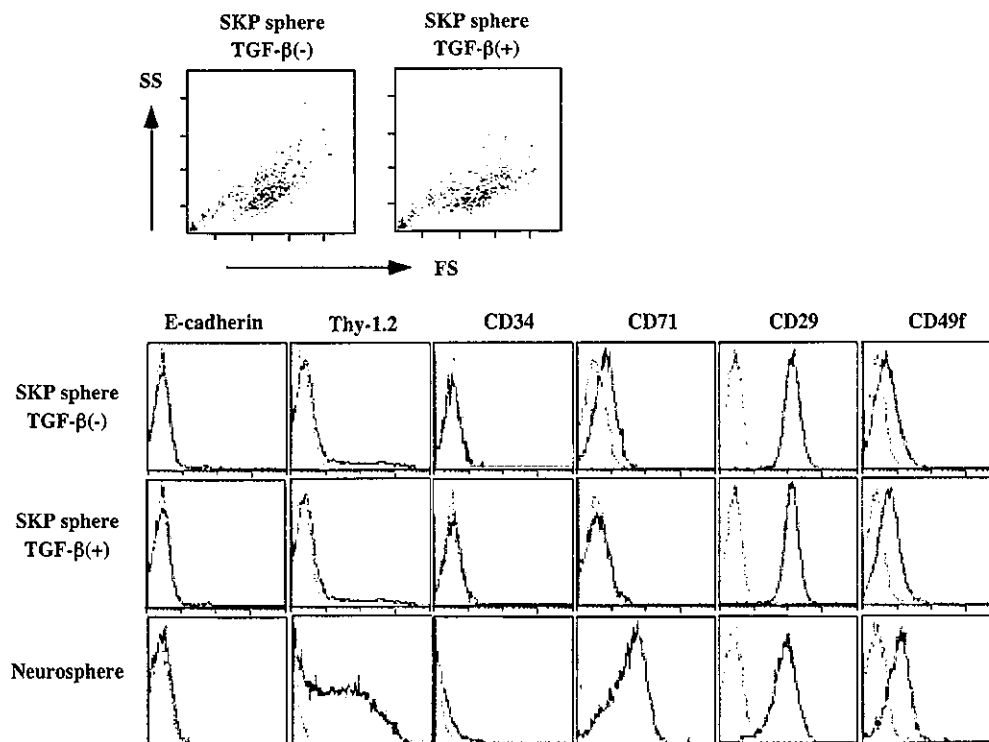


Fig. 7. TGF- $\beta$  does not alter the characteristic of the cells within colonies of SKPs, and SKPs differ from neurosphere colonies. The single cell suspensions from SKPs with or without TGF- $\beta$  and single cell suspensions from the secondary embryonic forebrain-derived neural stem cells were stained with antibodies against E-cadherin, CD34, CD71, CD29, and CD49f. The forward/side scatter of cells from sphere colonies with/without TGF- $\beta$  are also shown (top). Labeled cells were analyzed on a flow cytometer (solid lines). Dotted lines indicate negative control staining with an isotype antibody. The representative results from at least three independent experiments are shown.

Comparison of SKPs with neural stem cells

Next, we determined whether TGF- $\beta$  also facilitates the formation of neurospheres derived from embryonic striatal primordial-derived cells or whether the effect is rather more specific to SKPs. Although neurospheres were formed with EGF or bFGF alone, the combination of EGF and bFGF significantly increased the number of neurospheres by about 3.5-fold (Fig. 8A), similar to their behavior in previous studies [18] as well as to that of SKPs. However, TGF- $\beta$  reduced the number of neurosphere colonies and their diameter (Fig. 8B). These results suggest that SKPs differ from neurospheres in term of TGF- $\beta$  response.

We then analyzed the expression of cell-surface molecules in neurosphere colonies by flow cytometry. In contrast to SKPs, positive expression of Thy-1.2 was observed (Fig. 7, bottom), which was consistent with a previous study [19]. Furthermore, CD71 was also expressed in neural stem cells from neurosphere (Fig. 7, bottom). These results suggest that SKPs and neural stem cells express different sets of cell surface markers.

Age-independence for TGF- $\beta$  responsiveness in the formation and proliferation of the sphere

To study how aging affects the formation of sphere colonies and their response to TGF- $\beta$ , mice at the age of 3, 6, 12, 18, and 24 months were used for analysis. The number of the sphere colonies dramatically decreased with age, although TGF- $\beta$  significantly facilitated the formation of sphere colonies from the mice of all ages examined. The effect was most evident with 3-month-old mice (Fig. 9A).

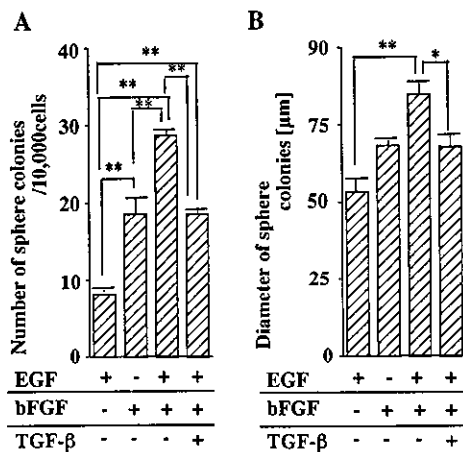


Fig. 8. TGF- $\beta$  does not affect neural stem cells derived from embryonic forebrain. The cells isolated from the embryonic striatum cells were plated at cell density of 10 cells/ $\mu$ l in 1 ml culture medium in 24-well dishes (10,000 cells/well). Media were supplemented with in medium with EGF, bFGF, or TGF- $\beta$ , or their combination. After 14 days in vitro, the number of primary sphere colonies per well (A,  $n = 3$ ) and their diameters (B,  $n > 10$ ) were measured (\* $P < 0.05$ , \*\* $P < 0.01$ ). The representative results from at least three independent experiments are shown.

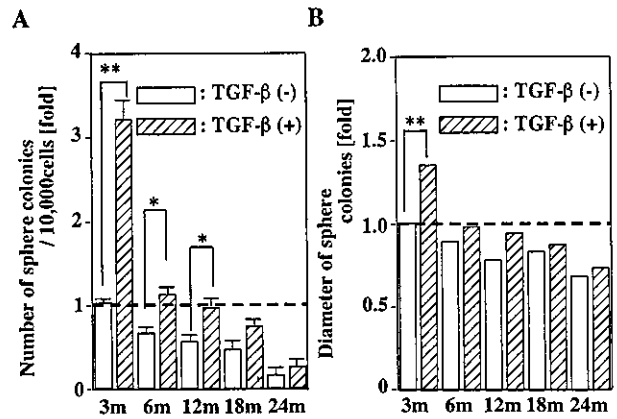


Fig. 9. TGF- $\beta$  facilitates sphere formation and proliferation independently of age. The cells isolated from the ear skin (3–24 months) were plated at cell density of 10 cells/ $\mu$ l in 1 ml culture medium in 24-well dishes (10,000 cells/well). After 14 days, the number of primary sphere colonies per well (A,  $n = 3$ ) and their diameters (B,  $n > 10$ ) were measured (\* $P < 0.05$ , \*\* $P < 0.01$ ). The representative results from at least three independent experiments are shown.

Additionally, although the diameters of the sphere colonies also decreased with age, the addition of TGF- $\beta$  increased the size of sphere colonies at all age (Fig. 9B). These results suggest that TGF- $\beta$  increased the sphere colony formation and proliferation independently of age.

Discussion

In this study, we have isolated sphere colonies from the skin using the sphere forming culture established by Toma et al. [13], in which cells that grow in suspension can be selected. Similar to their observations of the SKPs [13], these sphere colonies expressed nestin and fibronectin and differentiated to neuron, glia, smooth muscle cells, and adipocytes. We have passaged these cells up to 12 months without senescence until now. We could also obtain sphere colonies from skins from other sites including the abdomen and the back; however, the cells from the ear skin were separated more easily therefore sphere colonies from the ear skin were analyzed in the present study. Nonetheless, our results confirmed the existence in the skin of sphere-forming cells with multi-lineage potency for differentiation. Furthermore, we have established a clonal culturing system for SKPs without aggregation of the cells, using methylcellulose-added medium, as described for neurosphere formation [17].

Our results demonstrated that the numbers and sizes of the sphere colonies significantly increased with the addition of TGF- $\beta$ , while the expression of marker proteins and the potency of differentiation remained unaffected. Because EGF or bFGF was indispensable for SKP sphere formation, TGF- $\beta$  is likely to enhance the EGF and bFGF signaling pathways in SKPs, resulting in the increased number of the cells that initiated sphere formation as well as their proliferation. Interestingly, this positive effect of TGF- $\beta$  was not

observed in the neurosphere formation. Consistent with this, expression of several cell-surface markers also differed between neural stem cells and SKPs, although SKPs can differentiate into neuronal cells at a relatively high rate. These results collectively suggest that SKPs possess distinctive phenotypes from stem cells isolated from other tissues.

The origin of the cells in the skin that give rise to sphere colonies remains unknown. They may be an unidentified stem cell population in the dermis, while they may be generated through transdifferentiation of cells constituting the skin. The major cells of the skin include keratinocytes, fibroblasts, adipocytes, and endothelial cells. Although the effect of TGF- $\beta$  is not always the same, TGF- $\beta$  negatively regulates cell proliferation in general [20]. Most studies in vitro and in vivo support the hypothesis that TGF- $\beta$  inhibits the proliferation of basal keratinocytes [21–26]. Additionally, TGF- $\beta$  negatively regulates adipocytes differentiation in vitro and in vivo [27]. Furthermore, proliferation and migration of the endothelial cells in vivo and in vitro are inhibited by TGF- $\beta$  [28,29]. By contrast, TGF- $\beta$  can stimulate the proliferation of fibroblasts [30–32]. Therefore, among the major cells in the skin, only the growth of fibroblasts is shown to be positively regulated by TGF- $\beta$  signaling. While this may indicate that fibroblast-like cells give rise to skin-derived precursors, SKPs did not retain the characteristics of fibroblasts such as vimentin expression and collagen secretion (data not shown).

The numbers and sizes of sphere colonies were strikingly associated with the age of the mice, which may indicate the difficulties in applying SKPs to cell-based transplantation therapy as the target of the autologous cell-replacement would be elderly people in many cases. Nonetheless, this study demonstrated that TGF- $\beta$  increased the sphere formation independently of age, suggesting the possibility that improving the techniques of expanding stem cells can overcome this difficulty.

In summary, we have demonstrated that TGF- $\beta$  increases the formation and the proliferation of skin-derived stem cell colonies without affecting their potency of differentiation. Adult stem cells from the skin with the addition of TGF- $\beta$  during colony formation may become an accessible source for autologous cell-replacement therapy.

### Acknowledgments

We thank Dr. Kohei Miyazono for helpful discussions and Dr. Makoto Asashima for reagents. This work was supported by the Health Science Research Grant from the Japanese Ministry of Health, Labor, and Welfare.

### References

- [1] D.L. Clarke, C.B. Johansson, J. Wilbertz, B. Veress, E. Nilsson, H. Karlstrom, U. Lendahl, J. Frisen, Generalized potential of adult neural stem cells, *Science* 288 (2000) 1660–1663.
- [2] G.C. Kopen, D.J. Prockop, D.G. Phinney, Marrow stromal cells migrate throughout forebrain and cerebellum, and they differentiate into astrocytes after injection into neonatal mouse brains, *Proc. Natl. Acad. Sci. U. S. A.* 96 (1999) 10711–10716.
- [3] J. Sanchez-Ramos, S. Song, F. Cardozo-Pelaez, C. Hazzi, T. Stedeford, A. Willing, T.B. Freeman, S. Saporta, W. Janssen, N. Patel, D.R. Cooper, P.R. Sanberg, Adult bone marrow stromal cells differentiate into neural cells in vitro, *Exp. Neurol.* 164 (2000) 247–256.
- [4] D. Woodbury, E.J. Schwarz, D.J. Prockop, I.B. Black, Adult rat and human bone marrow stromal cells differentiate into neurons, *J. Neurosci. Res.* 61 (2000) 364–370.
- [5] G. Ferrari, G. Cusella-De Angelis, M. Coletta, E. Paolucci, A. Stornaiuolo, G. Cossu, F. Mavilio, Muscle regeneration by bone marrow-derived myogenic progenitors, *Science* 279 (1998) 1528–1530.
- [6] E. Lagasse, H. Connors, M. Al-Dhalimy, M. Reitsma, M. Dohse, L. Osborne, X. Wang, M. Finegold, I.L. Weissman, M. Grompe, Purified hematopoietic stem cells can differentiate into hepatocytes in vivo, *Nat. Med.* 6 (2000) 1229–1234.
- [7] C. Niemann, F.M. Watt, Designer skin: lineage commitment in post-natal epidermis, *Trends Cell Biol.* 12 (2002) 185–192.
- [8] F.M. Watt, Epidermal stem cells: markers, patterning and the control of stem cell fate, *Philos. Trans. R. Soc. Lond., B Biol. Sci.* 353 (1998) 831–837.
- [9] S. Ghazizadeh, L.B. Taichman, Multiple classes of stem cells in cutaneous epithelium: a lineage analysis of adult mouse skin, *EMBO J.* 20 (2001) 1215–1222.
- [10] G. Taylor, M.S. Lehrer, P.J. Jensen, T.T. Sun, R.M. Lavker, Involvement of follicular stem cells in forming not only the follicle but also the epidermis, *Cell* 102 (2000) 451–461.
- [11] P.A. Zuk, M. Zhu, H. Mizuno, J. Huang, J.W. Futrell, A.J. Katz, P. Benhaim, H.P. Lorenz, M.H. Hedrick, Multilineage cells from human adipose tissue: implications for cell-based therapies, *Tissue Eng.* 7 (2001) 211–228.
- [12] P.A. Zuk, M. Zhu, P. Ashjian, D.A. De Ugarte, J.I. Huang, H. Mizuno, Z.C. Alfonso, J.K. Fraser, P. Benhaim, M.H. Hedrick, Human adipose tissue is a source of multipotent stem cells, *Mol. Biol. Cell* 13 (2002) 4279–4295.
- [13] J.G. Toma, M. Akhavan, K. Fernandes, F. Barnabe-Heider, A. Sadikot, D.R. Kaplan, F.D. Miller, Isolation of multipotent adult stem cells from the dermis of mammalian skin, *Nat. Cell Biol.* 3 (2001) 778–784.
- [14] M. Okabe, M. Ikawa, K. Kominami, T. Nakanishi, Y. Nishimune, 'Green mice' as a source of ubiquitous green cells, *FEBS Lett.* 407 (1997) 313–319.
- [15] B.A. Reynolds, W. Tetzlaff, S. Weiss, A multipotent EGF-responsive striatal embryonic progenitor cell produces neurons and astrocytes, *J. Neurosci.* 12 (1992) 4565–4574.
- [16] F.H. Gage, P.W. Coates, T.D. Palmer, H.G. Kuhn, L.J. Fisher, J.O. Suhonen, D.A. Peterson, S.T. Suhr, J. Ray, Survival and differentiation of adult neuronal progenitor cells transplanted to the adult brain, *Proc. Natl. Acad. Sci. U. S. A.* 92 (1995) 11879–11883.
- [17] A. Gritti, E.A. Parati, L. Cova, P. Frolichsthal, R. Galli, E. Wanke, L. Faravelli, D.J. Morassutti, F. Roisen, D.D. Nickel, A.L. Vescovi, Multipotent stem cells from the adult mouse brain proliferate and self-renew in response to basic fibroblast growth factor, *J. Neurosci.* 16 (1996) 1091–1100.
- [18] P. Taupin, J. Ray, W.H. Fischer, S.T. Suhr, K. Hakansson, A. Grubb, F.H. Gage, FGF-2-responsive neural stem cell proliferation requires CCG, a novel autocrine/paracrine cofactor, *Neuron* 28 (2000) 385–397.
- [19] W. Vogel, F. Grunebach, C.A. Messam, L. Kanz, W. Brugger, H.J. Buhning, Heterogeneity among human bone marrow-derived mesenchymal stem cells and neural progenitor cells, *Haematologica* 88 (2003) 126–133.
- [20] K. Miyazono, Positive and negative regulation of TGF-beta signaling, *J. Cell Sci.* 113 (2000) 1101–1109.

- [21] E. Fuchs. Epidermal differentiation: the bare essentials, *J. Cell Biol.* 111 (1990) 2807–2814.
- [22] J.A. Pietenpol, J.T. Holt, R.W. Stein, H.L. Moses. Transforming growth factor beta 1 suppression of *c-myc* gene transcription: role in inhibition of keratinocyte proliferation, *Proc. Natl. Acad. Sci. U. S. A.* 87 (1990) 3758–3762.
- [23] M. Reiss, A.C. Sartorelli. Regulation of growth and differentiation of human keratinocytes by type beta transforming growth factor and epidermal growth factor, *Cancer Res.* 47 (1987) 6705–6709.
- [24] G.D. Shipley, M.R. Pittelkow, J.J.J. Wille, R.E.a. Scott, H.L. Moses. Reversible inhibition of normal human prokeratinocyte proliferation by type beta transforming growth factor-growth inhibitor in serum-free medium, *Cancer Res.* 46 (1986) 2068–2071.
- [25] R.F. Tucker, G.D. Shipley, H.L. Moses, R.W. Holley. Growth inhibitor from BSC-1 cells closely related to platelet type beta transforming growth factor, *Science* 226 (1984) 705–707.
- [26] X.J. Wang, D.A. Greenhalgh, J.R. Bickenbach, A. Jiang, D.S. Bundman, T. Krieg, R. Derynck, D.R. Roop. Expression of a dominant-negative type II transforming growth factor beta (TGF-beta) receptor in the epidermis of transgenic mice blocks TGF-beta-mediated growth inhibition, *Proc. Natl. Acad. Sci. U. S. A.* 94 (1997) 2386–2391.
- [27] R.A. Ignatz, J. Massague. Type beta transforming growth factor controls the adipogenic differentiation of 3T3 fibroblasts, *Proc. Natl. Acad. Sci. U. S. A.* 82 (1985) 8530–8534.
- [28] R. Frank, B.C. Adelman-Grill, K. Herrmann, U.F. Haustein, J.B. Petri, M. Heckmann. Transforming growth factor-beta controls cell-matrix interaction of microvascular dermal endothelial cells by downregulation of integrin expression, *J. Invest. Dermatol.* 106 (1996) 36–41.
- [29] G. Muller, J. Behrens, U. Nussbaumer, P. Bohlen, W. Birchmeier. Inhibitory action of transforming growth factor beta on endothelial cells, *Proc. Natl. Acad. Sci. U. S. A.* 84 (1987) 5600–5604.
- [30] K. Foitzik, R. Paus, T. Doetschman, G.P. Dotto. The TGF-beta2 isoform is both a required and sufficient inducer of murine hair follicle morphogenesis, *Dev. Biol.* 212 (1999) 278–289.
- [31] A.B. Roberts, M.B. Sporn, R.K. Assoian, J.M. Smith, N.S. Roche, L.M. Wakefield, U.I. Heine, L.A. Liotta, V. Falanga, J.H. Kehrl. Transforming growth factor type beta: rapid induction of fibrosis and angiogenesis in vivo and stimulation of collagen formation in vitro, *Proc. Natl. Acad. Sci. U. S. A.* 83 (1986) 4167–4171.
- [32] M.B. Sporn, A.B. Roberts. Transforming growth factor-beta: recent progress and new challenges, *J. Cell Biol.* 119 (1992) 1017–1021.



# An in vitro outgrowth culture system for normal human keratinocytes

Hironobu Ura\*, Fujie Takeda, Hitoshi Okochi

Department of Tissue Regeneration, Research Institute, International Medical Center of Japan, 1-21-1 Toyama, Shinjuku-Ku, Tokyo 162-8655, Japan

Received 17 September 2003; received in revised form 6 February 2004; accepted 1 March 2004

## KEYWORDS

Calcium;  
Keratinocytes;  
Stress, mechanical;  
Wound healing

**Summary Background:** Normal human epidermal keratinocytes usually proliferate in low-calcium and differentiate in high-calcium without a feeder layer, but they stop proliferating and differentiate at confluency even in low-calcium, serum-free medium. **Objective:** We speculated that this contact inhibition would be mediated in part by mechanical tension. To prove this, we created a new assay system. **Methods:** A 10 mm diameter cloning ring was put on the center of a 60 mm dish coated with type I collagen. Keratinocytes were plated in the ring and incubated for 4 h, then we had a circular epidermal monolayer sheet. We changed the mechanical tension by removing the ring and measured the diameter of the sheet under various conditions. **Results:** When we used keratinocyte-serum free medium (SFM) whose calcium concentration is below 0.1 mM as a medium, the keratinocytes in the perimeter migrated individually, and the keratinocytes in the center portion started differentiation. However, when we added calcium chloride to SFM (final concentration more than 0.5 mM), keratinocytes at the periphery showed marked lamellipodia without losing contact with the surrounding cells. These keratinocytes showed coordinate sheet-like outgrowth as a whole even in high concentrations of calcium. **Conclusion:** These results suggest that other than calcium concentration, change of the mechanical tension would be one of the factors that mediate proliferation or differentiation of keratinocytes and that this new assay can be useful in analyzing proliferation, differentiation, and migration of keratinocytes.

© 2004 Japanese Society for Investigative Dermatology. Published by Elsevier Ireland Ltd. All rights reserved.

## 1. Introduction

Keratinocyte cultivation has been studied since the 1970's. Human epidermal keratinocytes grow from single cells into colonies [1]. From then, a variety of agents were studied as modifiers of terminal differ-

entiation of keratinocytes. For example epidermal growth factor (EGF) delays senescence of the cells by maintaining them in a state further removed from terminal differentiation [2].

Calcium has been thought to be the most important factor which influences proliferation and differentiation of keratinocytes. When medium calcium is lowered to 0.05–0.1 mM, mouse keratinocytes proliferate rapidly with a high growth fraction, do not stratify, and they grow as a monolayer for several months [3]. An improved

\*Corresponding author. Tel.: +81-3-3202-7181;

fax: +81-3-3207-1038.

E-mail address: hura@imc.hosp.go.jp (H. Ura).

serum-free culture system without a feeder layer has been developed for human epidermal keratinocytes and a high-calcium concentration (1.0 mM) induces stratification and terminal differentiation [4]. On the other hand, keratinocytes stop proliferating and begin to differentiate at confluency even in low calcium concentration. We speculated that other than calcium concentration, change of the mechanical tension would be one of the factors that mediate proliferation or differentiation of keratinocytes. To prove this, we created a new system modifying the conventional outgrowth culture system.

It is well known that an outgrowth culture can be done by *ex vivo* culture of various epithelial tissues [5,6]. In those systems, fibroblasts also grow as well as epithelial cells. Keratinocyte outgrowth has been studied using an *in vitro* agarose gel keratinocyte outgrowth system [7] or keratinocyte–collagen gel composite model [8]. Keratinocytes can grow from single cell to form a colony in the presence of a feeder layer [9]. Herein we describe a keratinocyte-only outgrowth culture system without a feeder layer which enables us to perform both quantitative and qualitative analyses.

## 2. Materials and methods

### 2.1. Media

Dulbecco's minimal Eagle's medium (DMEM) (catalog no. 11885084, Invitrogen, Calsbad, CA) was supplemented with 10% fetal bovine serum (FBS), penicillin (5 U/ml), and streptomycin (5 µg/ml) (all from Invitrogen). Serum-free DMEM was used in some experiments.

Keratinocyte-serum free medium (SFM) (catalog no. 10724011, Invitrogen) was supplemented with epidermal growth factor (EGF) (5 ng/ml), bovine pituitary extract (50 µg/ml), penicillin (5 U/ml), and streptomycin (5 µg/ml) (all from Invitrogen).

In some experiments, calcium chloride was added to SFM to adjust the calcium concentration to 0.5 mM, 1.0 mM or 1.5 mM. EGF was omitted in other experiments. DMEM:SFM (1:3) mixture was also used in some experiments.

### 2.2. Cell culture and preparation of the keratinocyte sheets

Normal human epidermal keratinocytes derived from neonatal foreskin (Bio Whittaker, Walkersville, MD) were cultured, and from first to

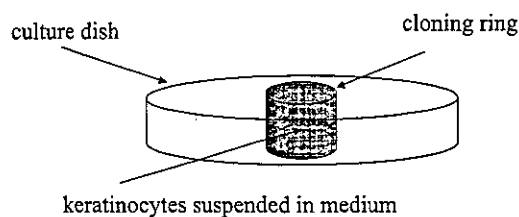


Fig. 1 Scheme of the assay. The standard experiment was performed by plating  $15 \times 10^4$  keratinocytes suspended in 200 µl keratinocyte-SFM onto a type I collagen-coated 60 mm culture dish inside a 10 mm cloning ring and the ring was removed after 4 h of incubation.

third passage cells were used for experiments. An excessive amount of keratinocytes suspended in keratinocyte-SFM were plated in a cloning ring (Iwaki, Tokyo, Japan) (standard plating density;  $15 \times 10^4$  keratinocytes suspended in 200 µl medium in 10 mm ring) onto the center of each culture dish (Biocoat Collagen I, Collagen IV, Laminin or Human Fibronectin Cellware 60 mm Dish) (Becton Dickinson, Franklin Lakes, NJ) or Glass Base Dish (Iwaki, Tokyo, Japan) and incubated in a humidified 5% CO<sub>2</sub> atmosphere at 37 °C (Fig. 1). Consequently, a circular monolayer sheet of keratinocytes was formed. After the ring was removed and 5 ml medium (DMEM:SFM (1:3) mixture was used in the standard experiment) was poured in the dish, the keratinocyte sheet began to grow concentrically. The medium was changed every 2–3 days.

### 2.3. Analyzing keratinocyte outgrowth

We measured the diameter of the sheet under various conditions. Several factors were examined, including the interval between plating the cells and removing the ring, the number of keratinocytes plated in the ring, the diameter of the ring, coating materials of the dishes, and the kind of medium.

In order to measure the diameter of the keratinocyte sheet, we provided various sized circles at intervals of 1 mm on transparent films, then laid them under the dishes under an inverted microscope. We searched the pre-described circle which fitted each keratinocyte sheet best, and regarded it as the diameter of the sheet. If the sheet was an ellipse form, we regarded the major axis as the diameter of the sheet.

To examine the differentiation of the sheet, immunofluorescence study was performed. The keratinocyte sheet was rinsed three times with phosphate buffered saline (PBS) and fixed with methanol on day 9. The fixed sheet was rinsed

with PBS and blocked with bovine serum albumin (Nacalai Tesque Inc., Kyoto, Japan). The sheet was then rinsed with PBS and incubated with primary antibody: mouse anti-cytokeratin10 (Chemicon International, Inc., CA) for 2 h at 37 °C at a dilution 1:250, washed with PBS and incubated with the fluorophore conjugated secondary antibody: Alexa Fluor 594 (goat anti-mouse IgG, Molecular Probes, Inc., OR) for 1 h at 37 °C at a dilution 1:400. Stained sheet was mounted and examined with a fluorescent microscope.

To observe mitotic activity, the keratinocyte sheet was pulse-labeled on day 1 and day 4 of culture with 10  $\mu$ M 5-bromo-2'-deoxyuridine (BrdU) obtained from In Situ Cell Proliferation Kit, FLUOS (Cat. No. 1 810 740) (Roche Diagnostics Corporation Indianapolis, IN). In this experiment, keratinocytes were plated in a cloning ring which was put on Collagen-I coated cover glass 25 mm type (Iwaki, Tokyo, Japan), which was laid on Glass Base Dish (Iwaki, Tokyo, Japan). Cells were incubated with BrdU for 2 h, washed three times with PBS, and fixed. Fixation was performed with a fixative solution made up of 70% ethanol in 50 mM glycine buffer pH 2.0 for 45 min at room temperature, after which the sheet was incubated in 4 M hydrochloric acid for 15 min at room temperature. Keratinocytes were immunostained using a monoclonal BrdU antibody obtained from In situ Cell Proliferation Kit, FLUOS (Cat. No. 1 810 740) (Roche Diagnostics Corporation Indianapolis, IN) as the primary antibody, followed by the biotinylated secondary antibody obtained from the Vectastain Universal Elite ABC Kit (Vektor Labs., Burlingame, CA) as described by the supplier. Immunostained cells were visualized using DAKO Envision Kit (DAKO, Carpinteria, CA).

We calculated the BrdU-labeling index (BrdU-LI) to analyze mitotic activity quantitatively. BrdU-LI is a proportion of BrdU positive cells in all cells. We counted BrdU positive cells and negative cells in ten fields (about 500 cells in total) under microscope at 400 $\times$  high power field both in the center and periphery of the sheet on day 1 and day 4, then calculated the average and standard errors of BrdU-LI.

#### 2.4. Inhibitors of keratinocyte outgrowth

Cytochalasin D (an inhibitor of actin polymerization) (Calbiochem, Darmstadt, Germany) diluted in dimethyl sulfoxide (DMSO) at the concentration of 1  $\mu$ g/ml and AG1478 (an inhibitor of epidermal growth factor receptor kinase) (Calbiochem) at the concentration of 0 M, 200 nM and 2  $\mu$ M were used as inhibitors of the growth of keratinocytes.

#### 2.5. Statistical analysis

Results are presented as mean values and standard errors. Significant differences were calculated using the Student *t*-test. A *P*-value of less than 0.05 was considered as statistically significant. All analyses were performed with Excel software.

### 3. Results

#### 3.1. The form of the keratinocyte sheet

When we used SFM with a calcium concentration below 0.1 mM as the medium, the keratinocytes in the perimeter migrated individually, and the keratinocytes in the center portion started differentiation (Fig. 2A and B), which was confirmed by the immunostaining with cytokeratin10 (Fig. 2E and F). The migrating edge was also positive for cytokeratin10 (data not shown). However, when we added calcium chloride to SFM at a final concentration of more than 0.5 mM, keratinocytes at the periphery showed marked lamellipodia without losing contact with the surrounding cells. These keratinocytes showed coordinated sheet-like outgrowth as a whole (Fig. 2C and D). The sheet showed negative immunostaining for cytokeratin10 (data not shown).

#### 3.2. Factors which influence keratinocyte outgrowth

The time interval between plating keratinocytes into the ring onto a type I collagen-coated dish and removing the ring was changed to 4 h, 8 h, 12 h, or 16 h, but there were no differences in the growth rates of the sheets. After a few days, the diameter of the sheet increased 4 mm/day constantly for several days (data not shown).

Varying numbers of keratinocytes ( $5 \times 10^3$ ,  $1 \times 10^4$ ,  $2 \times 10^4$  or  $4 \times 10^4$ ) were plated in the 5 mm ring onto a type I collagen-coated dish. As the number of keratinocytes plated increased, the larger the diameter of the sheet became, but the rate of enlargement became constant after a few days (Fig. 3A).

The diameter of the ring (10 mm, 7 mm, 5 mm, or 3.4 mm) was examined. To adjust the plating density,  $15 \times 10^4$  keratinocytes in 200  $\mu$ l medium were plated in the 10 mm ring,  $7.5 \times 10^4$  keratinocytes in 100  $\mu$ l medium were plated in the 7 mm ring,  $3.7 \times 10^4$  keratinocytes in 50  $\mu$ l medium were plated in the 5 mm ring, and  $1.8 \times 10^4$  keratinocytes in 25  $\mu$ l medium were plated in the 3.4 mm ring

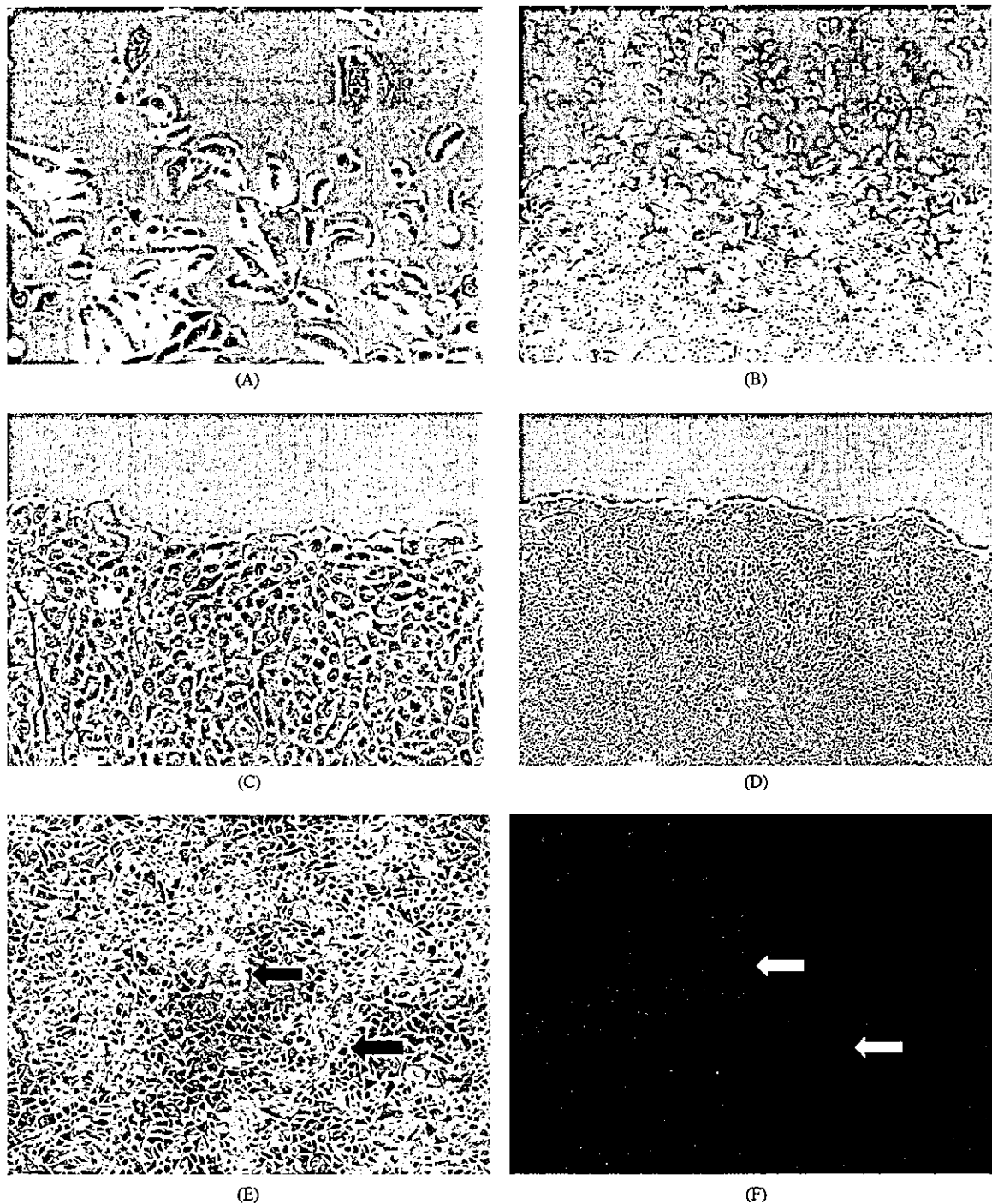


**Fig. 2** (A)–(D) The form of the keratinocyte sheet,  $15 \times 10^4$  keratinocytes were plated in 10 mm ring on a type I collagen-coated 60 mm dish and the ring was removed after 4 h of incubation. (A, B) The phase contrast microscopic image of the perimeter of the keratinocyte sheet 4 day after removing the ring when we used keratinocyte-SFM with a calcium concentration less than 0.1 mM as the medium. (C, D) The similar image taken when we added calcium chloride to SFM (final concentration more than 0.5 mM). Magnifications,  $\times 100$  (A, C),  $\times 40$  (B, D). (E, F) Immunofluorescence study with cytokeratin 10,  $15 \times 10^4$  keratinocytes were plated in 10 mm ring on a type I collagen-coated 60 mm dish and the ring was removed after 4 h of incubation. (E) The phase contrast microscopic image of the keratinocyte sheet 9 day after removing the ring when we used keratinocyte-SFM with a calcium concentration less than 0.1 mM as the medium. (F) The fluorescent microscopic image of the same field. Areas which look like whitish veils (black arrows in E) were positive for cytokeratin10 (white arrows in F). Magnification,  $\times 100$ .



onto a type I collagen-coated dish. The larger the diameter of the ring, the larger the diameter of the sheet became, but the rate of enlargement became constant after a few days (Fig. 3B).

Coating materials of the dishes were also varied in another series of experiments. The diameter of the sheet became larger in the following order, type

I collagen, type IV collagen, fibronectin, and laminin (Fig. 3C). The diameter of the sheet did not enlarge well on Glass Base Dish (Iwaki, Tokyo, Japan) (Fig. 3D).

Various media were also tested. When SFM (whose calcium concentration was adjusted to 0.5, 1.0 or 1.5 mM by adding calcium chloride) was

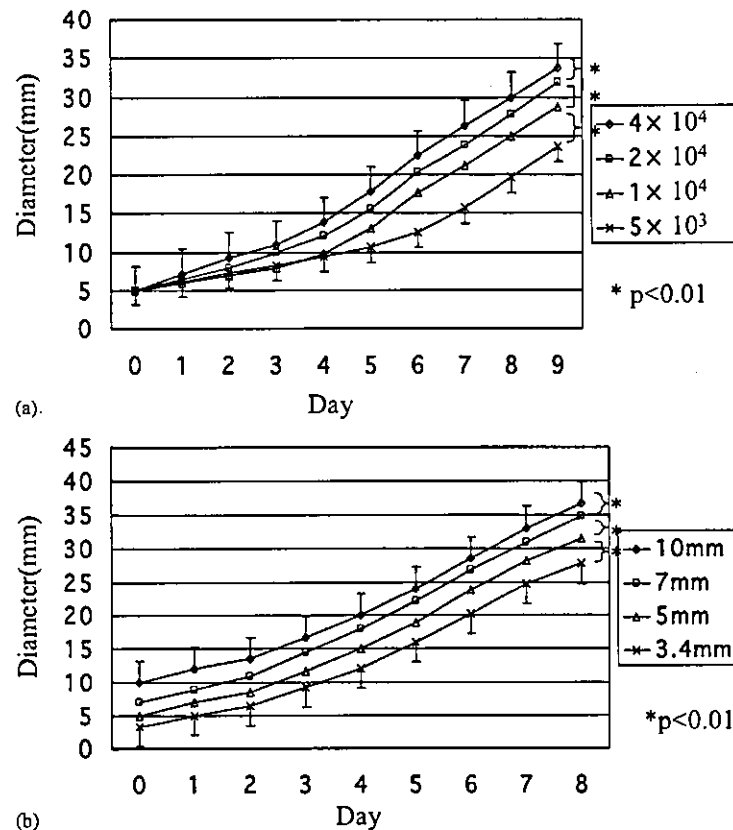


**Fig. 3** Factors affecting the keratinocyte outgrowth. The diameter of the keratinocyte sheet was observed as a function of time under various conditions. The ring was removed at day 0. Each point represents the mean size  $\pm$  S.E. of two or three sheets. (A) Various plating cell densities were examined. Keratinocytes suspended in 50  $\mu$ l medium were plated in 5 mm ring at a concentration of  $4 \times 10^4$ ,  $2 \times 10^4$ ,  $1 \times 10^4$  or  $5 \times 10^3$  on a type I collagen-coated 60 mm dish and the ring was removed after 4 h of incubation. DMEM:SFM (1:3) mixture was used as the medium. The diameter of the sheet was significantly different from each other at day 9 ( $P < 0.01$ ). (B) Various ring sizes were examined,  $15 \times 10^4$ ,  $7.5 \times 10^4$ ,  $3.7 \times 10^4$ , or  $1.8 \times 10^4$  keratinocytes suspended in medium were plated in a 10 mm, 7 mm, 5 mm, or 3.4 mm ring respectively, on a type I collagen-coated 60 mm dish and the ring was removed after 4 h of incubation. DMEM:SFM (1:3) mixture was used as the medium. The diameter of the sheet was significantly different from each other at day 8 ( $P < 0.01$ ). (C) Various coating materials were examined; type I collagen, type IV collagen, fibronectin and laminin were tested,  $15 \times 10^4$  keratinocytes were plated in 10 mm ring on each 60 mm dish and the ring was removed after 4 h of incubation. DMEM:SFM (1:3) was used as the medium. The diameter of the sheet was significantly different from each other at day 9 ( $P < 0.01$ ). (D) Type I collagen and glass base dish were compared.  $3.7 \times 10^4$  keratinocytes were plated in 5 mm ring on each dish and the ring was removed after 4 h of incubation. DMEM:SFM (1:3) was used as the medium. The diameter of the sheet on type I collagen-coated dish was significantly larger than that on glass base dish at day 4 ( $P < 0.01$ ). (E) Various culture media were examined. FBS-supplemented D:S (1:3) mixture, serum-free D:S (1:3) mixture, and S only (whose calcium concentration was adjusted to 0.5 mM by adding calcium chloride) were tested.  $15 \times 10^4$  keratinocytes were plated in 10 mm ring on a type I collagen-coated 60 mm dish and the ring was removed after 4 h of incubation. The diameter of the sheet was significantly different between D:S (1:3) mixture, S only and serum-free D:S (1:3) mixture at day 9 ( $P < 0.01$ ). D: Dulbecco's modified eagle medium, S: keratinocyte-serum free medium, FBS: fetal bovine serum, Ca: calcium.

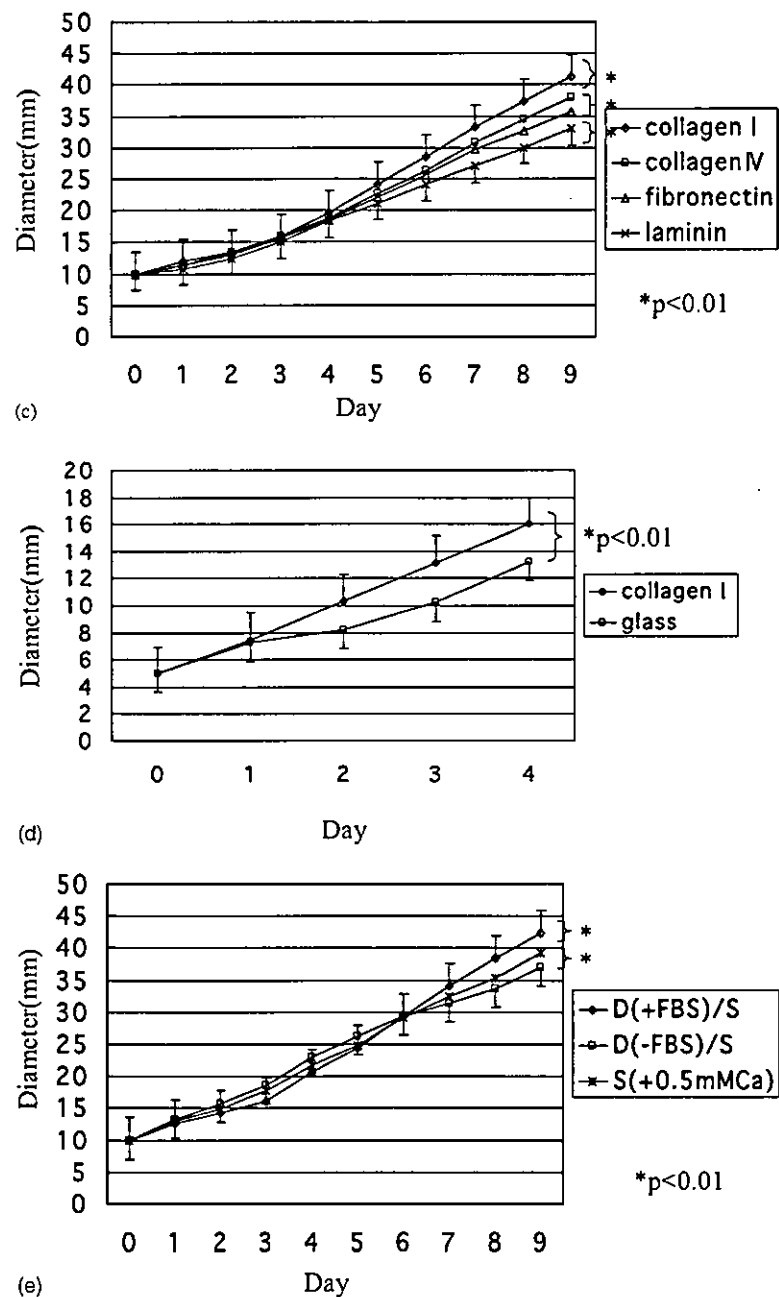


Fig. 3. (Continued).

used, there were no differences in the diameters of the sheet among the different concentrations of calcium. When DMEM:SFM (1:3) mixture was used, the diameter of the sheet was the smallest until day 5, but the largest after day 7. When the serum-free DMEM:SFM (1:3) mixture was used, the diameter of the sheet was the largest until day 5, but the smallest after day 7 (Fig. 3E).

Based on these results, the standard experiment was performed by plating  $15 \times 10^4$  keratinocytes in

10 mm ring, which was then placed on a type I collagen-coated 60 mm dish and removed after 4 h of incubation; DMEM:SFM(1:3) mixture was used as the medium.

### 3.3. Factors that inhibit keratinocyte outgrowth

The increase in the diameter of the sheet completely stopped, when cytochalasin D, which is an

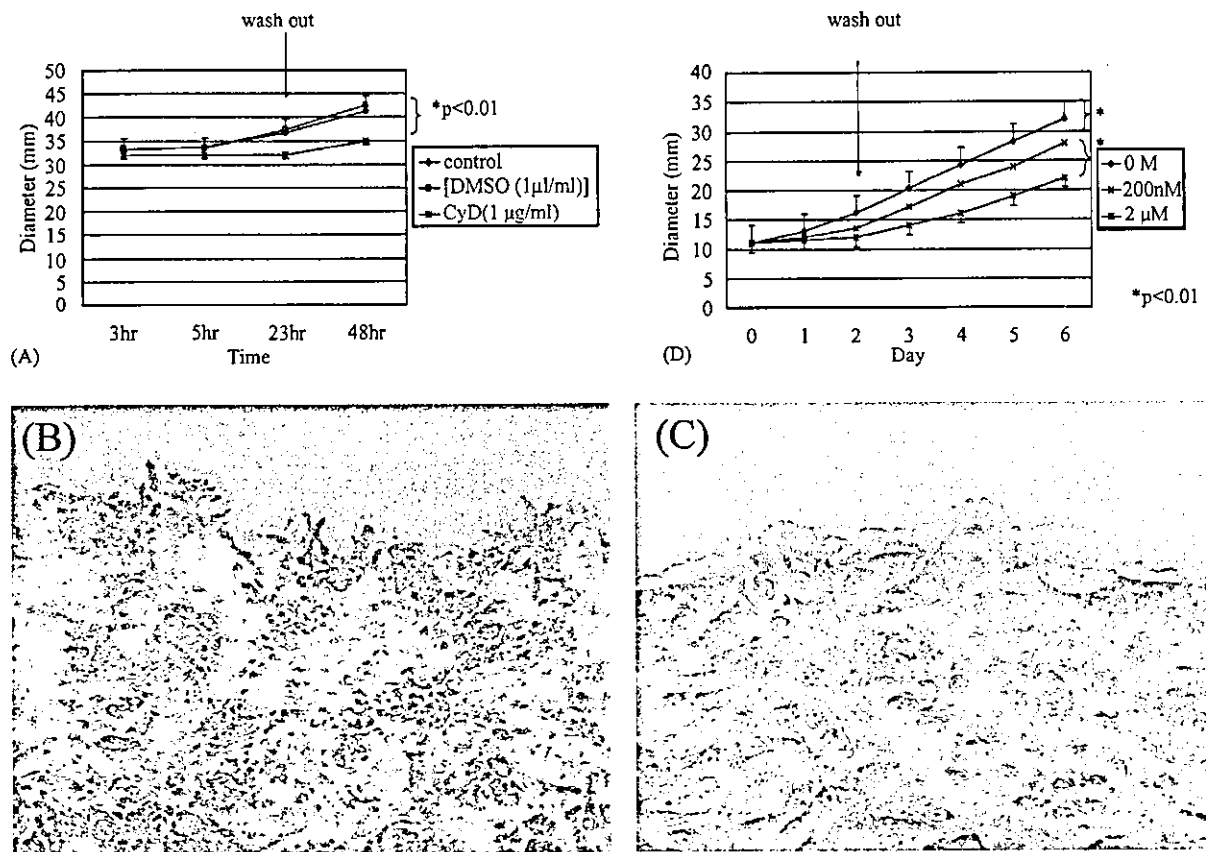


Fig. 4 Factors that inhibit keratinocyte outgrowth.  $15 \times 10^4$  keratinocytes were plated in 10 mm ring on a type I collagen-coated 60 mm dish and the ring was removed after 4 h of incubation. DMEM:SFM (1:3) was used as the medium. (A) The changes in the diameter of the keratinocyte sheet as a function of time were observed when cytochalasinD, which is an inhibitor of actin polymerization diluted in DMSO, was added at time 0 at the concentration of  $1 \mu\text{g/ml}$  and observed again after washing out the inhibitor. The diameter of the sheet when cytochalasin D was added was significantly smaller than that of control or when only DMSO was added at 48 h ( $P < 0.01$ ). Each point represents the mean size  $\pm$  S.E. of three sheets. (B, C) The phase contrast microscopic image of the perimeter of the keratinocyte sheet. (B) cytochalasinD was added. The magnification is,  $\times 200$ . (C) Only DMSO was added. The magnification is,  $\times 200$ . (D) The changes in the diameter of the keratinocyte sheet as a function of time were observed when AG1478, which is an inhibitor of EGF receptor kinase, was added at day 0 at the concentrations of 0 M, 200 nM and  $2 \mu\text{M}$ , and observed again after washing out the inhibitor. The diameter of the sheet was significantly different from each concentration of AG1478 at day 6 ( $P < 0.01$ ). Each point represents the mean size  $\pm$  S.E. of two sheets. CyD: cytochalasinD, DMSO: dimethyl sulfoxide. The magnification is,  $\times 200$ .

inhibitor of actin polymerization diluted in DMSO was added at the concentration of  $1 \mu\text{g/ml}$ , and it began to increase after washing out the inhibitor. When only DMSO was added ( $1 \mu\text{l/ml}$ ), the diameter of the sheet increased to the same degree as did the control (Fig. 4A). When cytochalasinD was added, the morphology of keratinocytes in the periphery of the sheet changed a great deal (Fig. 4B), as compared to those in the periphery, when only DMSO was added (Fig. 4C). When AG1478, which is an inhibitor of EGF receptor kinase, was added at the concentrations of 0 M, 200 nM and  $2 \mu\text{M}$ , the increase in the diameter of the sheet was inhibited in a manner dependent on concentration, and the

diameter began to increase again after the AG1478 was washed out (Fig. 4D). The diameter of the sheet was a little smaller when the DMEM:SFM (1:3) mixture without EGF was used than when the DMEM:SFM (1:3) mixture was used (data not shown).

### 3.4. The distribution of mitotic or proliferating cells in the sheet

The keratinocyte sheet was labeled with BrdU, then immunohistochemically stained with anti BrdU antibody, and the distribution of the mitotic or proliferating cells in the sheet was followed over time. When BrdU was used on day 1, more BrdU positive

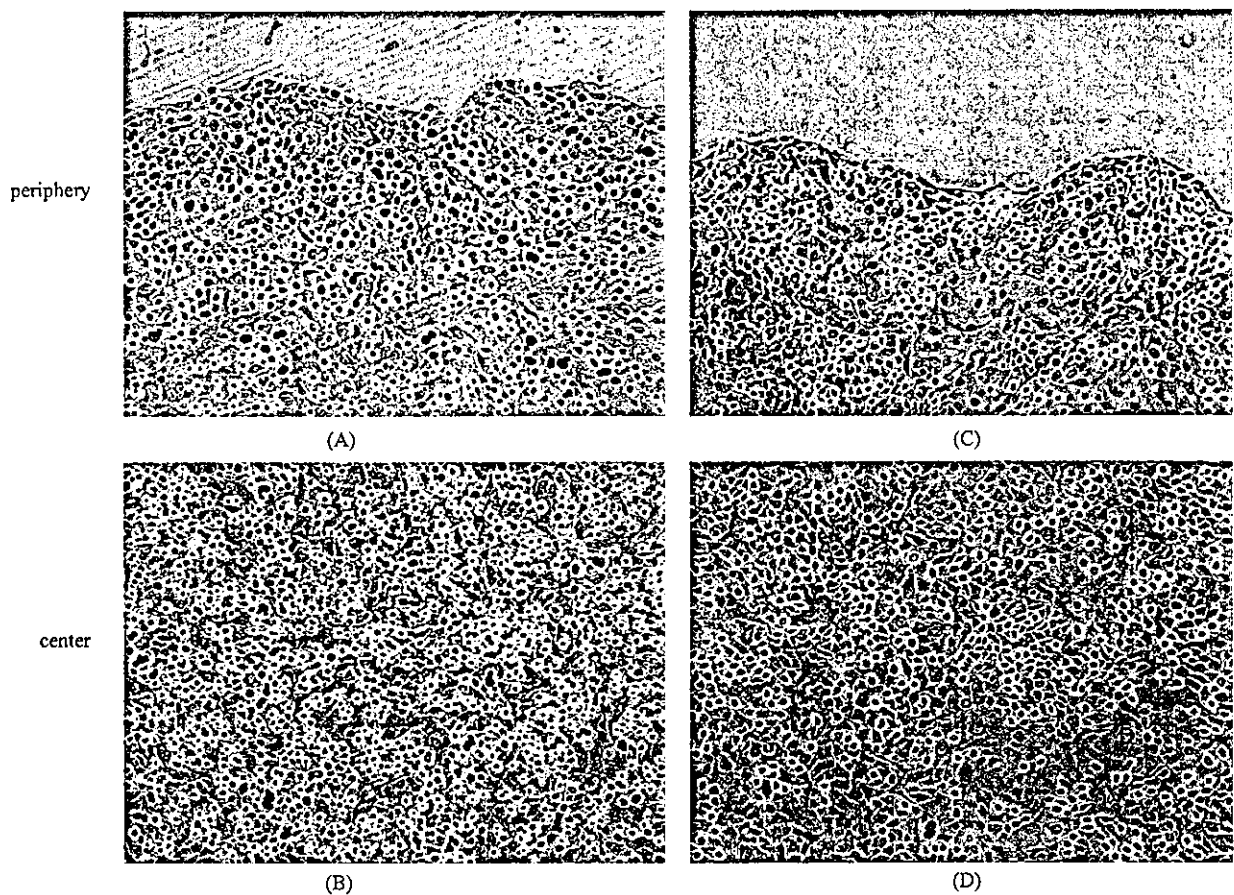


**Fig. 5** The distribution of the mitotic or proliferating cells in the sheet with time,  $15 \times 10^4$  keratinocytes were plated in 10 mm ring on a type I collagen-coated cover glass which was laid on a glass base dish and the ring was removed after 4 h of incubation. DMEM:SFM (1:3) was used as the medium. Keratinocyte sheets were labeled with BrdU on day 1 (A, B), or on day 4 (C, D). The magnification is,  $\times 400$ .

cells were seen in the center (BrdU-LI:  $66.1 \pm 2.4\%$ ) (Fig. 5B) than in the periphery (BrdU-LI:  $51.7 \pm 1.9\%$ ) (Fig. 5A) ( $P < 0.01$ ), but when BrdU was used on day 4, more BrdU positive cells were seen in the periphery (BrdU-LI:  $40.0 \pm 1.3\%$ ) (Fig. 5C) than in the center (BrdU-LI:  $33.9 \pm 6.5\%$ ) (Fig. 5D) ( $P < 0.05$ ).

#### 4. Discussion

We created a new outgrowth culture system for assay of normal human keratinocytes and examined the influences of calcium concentration, mechanical tension and other factors on sheet-form proliferation and differentiation of keratinocytes. At first, keratinocytes were plated in the cloning ring at confluency, and then we changed the mechanical tension by removing the ring. These keratinocytes showed coordinate sheet-like outgrowth, even in high concentrations of calcium. This is a very interesting finding, because in keratinocyte cultivation

without a feeder layer, switching from low to high calcium concentration induces differentiation [4]. In other words, we showed that the presence of a free end induces proliferation of keratinocytes even in high concentrations of calcium. We thought that other than calcium concentration, change of the mechanical tension would be one of the factors that mediate proliferation or differentiation of keratinocytes. In order to analyze further the effect of mechanical tension on the proliferation or differentiation of keratinocytes, further experiments are needed.

We then examined some factors that can influence or inhibit the keratinocyte outgrowth in order to explore how the keratinocytes sheet expands and found some interesting things. After a few days, the diameter of the sheet increased about 4 mm/day constantly for several days, independent of the plating cell density or the size of the ring. The diameter of the sheet did not enlarge well on bare glass, as compared with the dish coated with type I

collagen. This result suggests that keratinocytes may migrate, interacting with the components of the extracellular matrix.

Addition of cytochalasin D, an actin polymerization inhibitor, completely abolished keratinocyte outgrowth; after washing out the inhibitor, the keratinocytes resumed their outgrowth. A recent study showed that actin polymerization is the driving force for epithelial cell-cell adhesion [10]. Our results suggest that actin polymerization is also a driving force for this outgrowth.

EGF delays senescence of the cells by maintaining them in a state further removed from terminal differentiation [2]. The diameter of the sheet was a little smaller when EGF-free medium was used than when EGF-supplemented media was used. When AG1478, which is an inhibitor of EGF receptor kinase, was added, the inhibition of the increase in diameter of the sheet depended on inhibitor concentration, and the sheet began to increase in diameter after the AG1478 was washed out. These results suggest that signal transduction by EGF contributes to some degree to this outgrowth.

BrdU labeling experiments revealed that the distribution of BrdU positive cells gradually shifted from the center to the peripheral area. In other words, the mitotic or proliferating cells migrated from the center to the periphery along with the growth in the sheet. This phenomenon is compatible with the report that cells contributing to expansion of a large colony on a feeder layer are located close to the colony perimeter [9].

Wound re-epithelization usually has been studied by wounding animal skin [11–13]. In order to develop an in vitro model that is more similar to in vivo wound healing, we also attempted another technique, the 'ingrowth culture system', in which we plated keratinocytes outside the cloning ring onto the culture dish followed by removing the ring. This system failed because after removing the ring, some floating keratinocytes adhered to the empty center and started to proliferate, so that accurate quantitative analysis became impossible.

There have been reported some monolayer keratinocyte wound models, in which monolayer culture of keratinocytes is wounded with central scraping [14,15]. In these models, the wounds closed in order of hours, that is, analysis could be performed in only short duration. On the other hand, analysis could be performed in longer duration in our outgrowth system. In addition, a pipette tip was used to make wounds in the previous models, so there was a possibility that keratinocytes received some physical damages other than a free end and the change of mechanical tension, and such

physical damages could become cues of proliferation or migration of keratinocytes. On the other hand, removing the ring gives the change of mechanical tension and a free end but maybe less physical damages to keratinocytes. In such reasons, we thought that our outgrowth system is more suitable than the previous models in examining the effect of mechanical tension on keratinocytes and coordinate growth.

There also have been reported some methods to study the effect of mechanical tension on keratinocyte behaviour [16]. In these methods, stretching devices were used in which keratinocytes on the membrane can be extended. They can give the change of mechanical tension to some degree to keratinocytes, but there are no free ends, so they are not suitable for analyzing the migration of keratinocytes. We thought that one of the properties of our system is to focus on the change of mechanical tension in the wounded epidermis.

In conclusion, we established an in vitro outgrowth culture system without a feeder layer for normal human keratinocytes. In this system, removing the ring in vitro corresponds to inflicting a wound in vivo, because both events produce free edges leading to a change in the mechanical tension on the keratinocytes. This system also simulates an explant culture. This assay is useful for analyzing proliferation, or migration of keratinocytes and it could function as an in vitro model of keratinocyte kinetics in wound healing.

## Acknowledgements

This work was supported by the Health Science Research Grant from the Japanese Ministry of Health Labour and Welfare.

## References

- [1] Rheinwald JG, Green H. Serial cultivation of strains of human epidermal keratinocytes: the formation of keratinizing colonies from single cell. *Cell* 1975;6:331–44.
- [2] Rheinwald GJ, Green H. Epidermal growth factor and the multiplication of cultured human epidermal keratinocytes. *Nature* 1977;265:421–4.
- [3] Hennings H, Michael D, Cheng C, Steinert P, Holbrook K, Yuspa SH. Calcium regulation of growth and differentiation of mouse epidermal cells in culture. *Cell* 1980;19:245–54.
- [4] Boyc ST, Han RG. Calcium-regulated differentiation of normal human epidermal keratinocytes in chemically defined clonal culture and serum-free serial culture. *J Invest Dermatol* 1983;81:33s–40s.
- [5] Masui T. Establishment of an outgrowth culture system to study growth regulation of normal human epithelium. *In Vitro Cell Dev Biol Anim* 1995;31:440–6.

- [6] Mazzalupo S, Wawersik MJ, Coulombe PA. An ex vivo assay to assess the potential of skin keratinocytes for wound epithelialization. *J Invest Dermatol* 2002;118:866–70.
- [7] Grando SA, Crosby AM, Zelickson BD, Dahl MV. Agarose gel keratinocyte outgrowth system as a model of skin re-epithelialization: requirement of endogenous acetylcholine for outgrowth initiation. *J Invest Dermatol* 1993;101:804–10.
- [8] Tuan TL, Keller CL, Sun D, Nimni ME, Cheung D. Dermal fibroblasts activate keratinocyte outgrowth on collagens. *J Cell Sci* 1994;107:2285–9.
- [9] Barrandon Y, Green H. Cell migration is essential for sustained growth of keratinocyte colonies: the roles of transforming growth factor- $\alpha$  and epidermal growth factor. *Cell* 1987;50:1131–7.
- [10] Vasioukhin V, Bauer C, Yin M, Fuchs E. Directed actin polymerization is the driving force for epithelial cell–cell adhesion. *Cell* 2000;100:209–19.
- [11] Hammar H, Acevedo F, Naito S. Transferrin and epidermal growth. *Acta Derm Venereol Suppl (Stockh)* 1990;70:11–7.
- [12] Mellin TN, Cashen DE, Ronan JJ, Murphy BS, DiSalvo J. Acidic fibroblast growth factor accelerates dermal wound healing in diabetic mice. *J Invest Dermatol* 1995;104:850–5.
- [13] Onuma H, Matsui C, Morohashi M. Cell kinetic change during epidermal wound healing: Quantitative analysis using BrdU in the epidermal sheet. *Jpn J Dermatol* 1999;109:1015–9.
- [14] Yamada T, Aoyama Y, Owada MK, Kawakatsu H, Kitajima Y. Scraped-wounding causes activation and association of C-Src tyrosine kinase with microtubules in cultured keratinocytes. *Cell Struct Funct* 2000;25:351–9.
- [15] Providence KM, White LA, Tang J, Gonclaves J, Staiano-Coico L, Higgins PJ. Epithelial monolayer wounding stimulates binding of USF-1 to an E-box motif in the plasminogen activator inhibitor type 1 gene. *J Cell Sci* 2002;115:3767–77.
- [16] Kippenberger S, Bernd A, Loitsch S, Guschel M, Muller J, Bereiter-Hahn J, et al. Signaling of mechanical stretch in human keratinocytes via MAP kinases. *J Invest Dermatol* 2000;114:408–12.

Available online at [www.sciencedirect.com](http://www.sciencedirect.com)

SCIENCE @ DIRECT®

## Novel Collagen Sponge Reinforced with Polyglycolic Acid Fiber Produces Robust, Normal Hair in Murine Hair Reconstitution Model

M. ITOH,<sup>1,2</sup> Y. HIRAOKA,<sup>3</sup> K. KATAOKA,<sup>4</sup> N.H. HUH,<sup>4</sup> Y. TABATA,<sup>3</sup> and H. OKOCHI<sup>1</sup>

### ABSTRACT

The hair reconstitution assay is a useful system for studying cell–cell and epithelial–mesenchymal interaction. The current method consists of transplantation of both epidermal and dermal cells, using a silicone chamber placed on an athymic nude mouse. However, because of leakage and tilting of the grafted cells, the rate and area of hair growth vary depending on the chamber. We modified this method by using a collagen sponge as a scaffold and compared two types of collagen sponges, each having different tensile strengths. A conventional collagen sponge disturbed normal hair follicle formation; in contrast, a collagen sponge containing polyglycolic acid (PGA) fiber supported proper restructuring of skin and hair follicles. These data suggested the usefulness of PGA fiber-containing collagen sponges for hair reconstitution in research and clinical applications.

### INTRODUCTION

**H**AIR FOLLICLE FORMATION requires complex interactions of epidermal and dermal cells in a proper space.<sup>1–8</sup> Studies have demonstrated that epidermal multipotent stem cells in the bulge region of follicles are capable of generating every epithelial structure of hairy skin: keratinocytes, sebaceous glands, hair shafts, and hair follicles.<sup>9–12</sup> The dermal papilla cells of mesenchymal origin induce these epidermal stem cells to differentiate and develop into hair components.<sup>6–8</sup> Both the epidermal multipotent stem cells and the dermal papilla cells are indispensable for the proper growth of a hair. However, the precise cellular interactions in the hair formation remain unclear. To elucidate the mechanism, it is important to establish a model system for evaluating cellular interaction and molecular control in skin appendage formation.

Whereas *in vitro* reconstitution of hair follicles to date

has been unsuccessful, *in vivo* hair reconstitution assays, in which mixtures of several cells are transplanted in a silicone chamber onto the dorsal skin of athymic nude mice, have been frequently employed.<sup>4–8,13</sup> In the original method, the graft bed on the dorsal skin of the host mouse is prepared by inserting a ground glass disk between the skin and the thoracic wall. To make a better graft bed, the disk must be left in place for at least 3–4 weeks until a well-vascularized capsule of granulation tissue has formed around it. A silicone chamber is then attached onto the graft bed before transplantation.<sup>4–6,13</sup> Although the graft site is firmly fixed by adjusting such a graft bed in advance, this is complicated and time-consuming. Therefore, an alternative method has been developed, bypassing the process of disk insertion.<sup>7,8</sup> This simplified method, in which the thick cell suspensions are directly transferred onto the bare thoracic wall within the chamber, requires much skill and experience, because

<sup>1</sup>Department of Tissue Regeneration, Research Institute, International Medical Center of Japan, Tokyo, Japan.

<sup>2</sup>Department of Dermatology, Jikei University School of Medicine, Tokyo, Japan.

<sup>3</sup>Department of Biomaterials, Field of Tissue Engineering Institute for Frontier Medical Science, Kyoto University, Kyoto, Japan.

<sup>4</sup>Department of Cell Biology, Okayama University Graduate School of Medicine and Dentistry, Okayama, Japan.

the transferred cell mixture is apt to leak out and the grafted sites cannot be fixed with any certainty. We investigated the usage of scaffolds to solve these problems.

Various biodegradable polymers have been used as scaffolds for cellular proliferation and differentiation in tissue engineering.<sup>14</sup> As a collagen sponge (collagen being the main component of the extracellular matrix) has been extensively used because of its inherently superior cell affinity, we investigated whether it would be useful as a scaffold in the hair reconstitution assay. We created a novel collagen sponge reinforced by the incorporation of a bioabsorbable synthetic polymer, polyglycolic acid (PGA), which made it mechanically stronger. It seemed that the PGA(+) sponge would profit from the beneficial properties of both collagen and the synthetic polymer and found that it was indeed useful for hair reconstitution.

## MATERIALS AND METHODS

### *Collagen sponges*

Two types of collagen sponge, with and without PGA fibers, were prepared. Collagen sponges incorporating PGA fibers were fabricated by the conventional freeze-drying and dehydrothermal cross-linking methods. Briefly, a 3-mg/mL collagen solution (Nitta Gelatin, Osaka, Japan) was poured into a mold of PGA fiber (Gunze, Kyoto, Japan), 20  $\mu$ m in diameter, which had been homogeneously placed, followed by freeze-drying to obtain collagen sponges incorporating PGA fiber. The freeze-dried sponge was dehydrothermally cross-linked at 140°C for 12 h. A collagen sponge without PGA fibers was prepared similarly by using collagen solution alone.<sup>15</sup>

### *Morphological observation of collagen sponges*

The appearance and intrastucture of collagen sponges with or without PGA fiber incorporation were observed by scanning electron microscope (SEM) (S-2380N; Hitachi, Tokyo, Japan). The collagen sponges were cut with a razor blade. The cross-sections of sponge were coated with gold, using an ion sputter (E-1010; Hitachi) at 50 mtorr and 5 mA for 30 s and viewed by SEM at a voltage of 15 kV.

### *Animals and reagents*

C57BL/6J mice and athymic nude mice (BALB/cA Jcl-nu) were purchased from CLEA Japan (Shizuoka, Japan). Fetal mice were obtained from pregnant C57BL/6J mice at 16–17 days of pregnancy. Skin cells, isolated from fetal mice at this stage, retain the ability to form hair follicles in the reconstitution assay.<sup>13</sup> All studies were approved by the Animal Care Committee of the International Medical Center of Japan (Tokyo, Japan).

A Keratinocyte Growth Medium (KGM)-2 Bullet kit

was purchased from Cambrex Bio Science Walkersville (Walkersville, MD). KGM-A was prepared as recommended by the manufacturer. KGM-B is KGM-A without insulin, human epidermal growth factor, and bovine pituitary extract supplements.

### *Cell isolation*

The uterus was removed from each pregnant C57BL/6J mouse, and the individual fetuses were separated and washed in Dulbecco's phosphate-buffered saline (PBS; Sigma-Aldrich, St. Louis, MO). The full thickness of the dorsal skin was incised with small scissors, peeled from the subcutaneous tissue with forceps, and then incubated in KGM-B with 0.05% collagenase IV (Boehringer Ingelheim, Ingelheim, Germany) at 4°C for 15–16 h. The tissue was then split into epidermis and dermis, and these were dissociated by pipetting in KGM-A (for epidermis) or KGM-B (for dermis). The dissociated cells were filtered through a 70- $\mu$ m pore size nylon cell strainer. Each cell suspension was placed on ice until use.

### *Preparation of graft*

Two types of collagen sponge, with and without PGA fibers, were sterilized by gaseous sterilization beforehand. Because the PGA(+) collagen sponge was hydrophobic, it was rinsed with 70% ethanol, followed by washing in PBS and medium just before applying cell suspension.

Approximately  $1 \times 10^7$  cells in total, a combination of epidermal cells (about  $4 \times 10^6$ ) and dermal cells (about  $6 \times 10^6$ ) keeping the proportion of each isolated cell lineage, was centrifuged at 1000 rpm. Although it is possible to place approximately  $1 \times 10^6$  cells at least for hair reconstitution, it is necessary to prepare such numbers of cell for more consistent results. The resultant cell suspension (approximately 60  $\mu$ l) was evenly transferred to the collagen sponge.

### *Grafting*

A sterile silicone chamber was implanted into the back of 5 to 8-week-old athymic nude mice (BALB/cA Jcl-nu) to prevent cell migration from the adjacent skin (Fig. 1).<sup>13</sup> Briefly, after the mouse was anesthetized with an intraperitoneal injection (0.01–0.02 mL/g body weight) of 13% pentobarbital sodium (Dainippon Pharmaceutical, Osaka, Japan), a hole with a diameter of 1 cm was made in the dorsal skin. The lower part of the silicone chamber was then inserted between the skin and the thoracic wall and fixed by suturing. The collagen sponge was placed adjacent to the thoracic wall, and covered with the hat-shaped upper part of the chamber. One week after grafting, the upper part of the silicone chamber was removed. The lower part of the chamber was removed after 10–12 days, when the wound-healing process was completed.



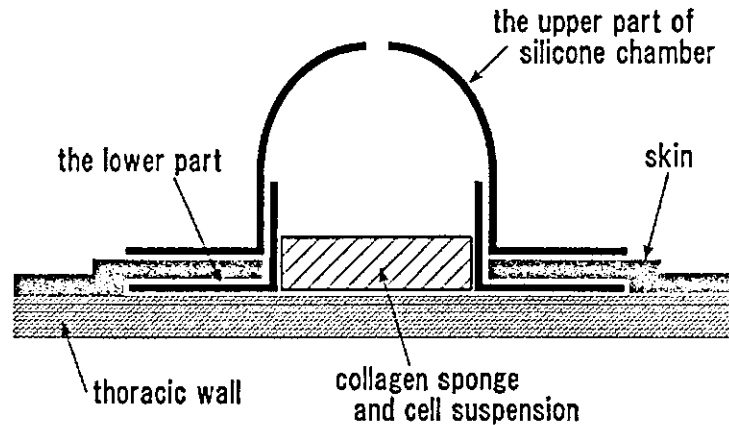


FIG 1. Scheme of the hair reconstitution assay, using a collagen sponge as the scaffold.

#### Evaluation of grafted sites

The grafts were observed daily for the first 10 days after grafting, and after that every other day for up to 3 weeks. Before the histological examination of the grafted sites, all hairs grown up from each grafted site were cut and spread on paper for counting. The graft site area was then measured to calculate the density of hair growth ( $n = 3$  for each group). For histological examination, the grafted sites were excised, fixed in 10% formaldehyde (Wako, Osaka, Japan) at room temperature for 1–2 h, and processed for paraffin sectioning. Histological sections (8  $\mu\text{m}$  thick) were stained with hematoxylin and eosin. Moreover, the number of epidermal cysts formed in the selected area of each grafted site was counted ( $n = 5$  for each group). The selected area was defined as an 80% area in the center of the middle section of a fixed grafted site.

## RESULTS

#### Appearance and intrastucture of collagen sponges

Figure 2 shows SEM photographs of cross-sections of collagen sponge with or without PGA fiber. Irrespective of the incorporated fiber, collagen sponge possessed an interconnected porous structure with an almost homogeneous pore size. Although PGA fibers were exposed in the pores of PGA-incorporated sponges, the internal structure was similar to that of sponge without PGA fibers.

#### Macroscopic analysis of grafted sites

To evaluate the effect of the conventional collagen PGA(-) sponge and PGA(+) sponge on the formation of

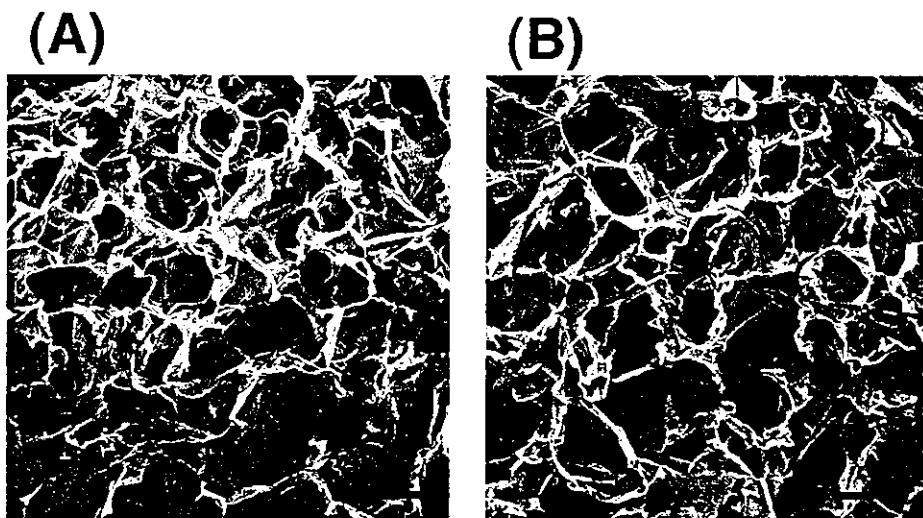
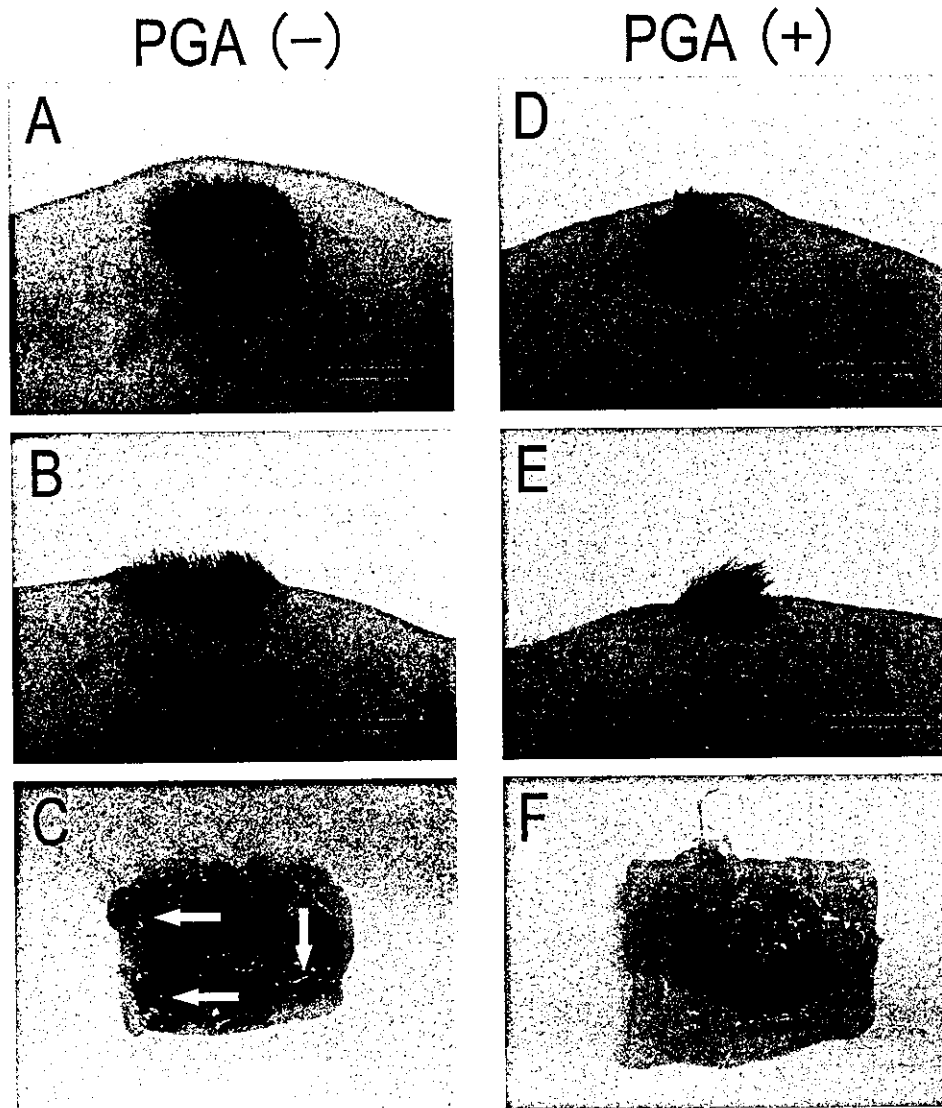


FIG 2. Cross-sectional SEM photographs of collagen sponge (A) and collagen sponge incorporating PGA fiber (B). Scale bars: 200  $\mu\text{m}$ .

hair in the reconstitution assay, we observed the appearance of the grafted sites for up to 3 weeks, when hair reconstitution is normally completed. On the grafted areas of the PGA(-) sponge, the hair follicles were observed for 1 week. However, the hair growth was poor and sparse, as shown in Fig. 3A and B. The size of the fixed grafted sites extended beyond the size of original sponge (Fig. 3A). Moreover, ectopic hair growth was seen macroscopically under the skin around the graft site (Fig. 3C).

When the grafts were made on a PGA(+) sponge, hair formation was induced 10–12 days after grafting, slightly later than on the PGA(-) sponge. However, the

hairs on the PGA(+) sponge were very thick and grew properly, compared with those on the PGA(-) sponge (Fig. 3D and E). Quantitative analysis of the hair density on each graft demonstrated that mean hair density was  $531 \pm 179$  and  $2808 \pm 1237$  hairs/cm<sup>2</sup> on PGA(-) and PGA(+) sponge, respectively (Fig. 4A). The size and shape of the grafted sites on the PGA(+) sponge stayed unchanged in comparison with the original sponge size. Little ectopic hair growth was noted (Fig. 3F). Moreover, hair and hair follicles grafted on the athymic mice were maintained for 6 months at least. Collectively, these data suggest that the PGA(+) sponge is more advantageous for hair growth.



**FIG 3.** Macroscopic appearance of the grafted sites on PGA(-) sponge (A–C) and PGA(+) sponge (D–F). (A and D) Overview; (B and E) lateral view; (C and F) back side of the grafted site. Much ectopic hair formation (arrows) was seen under the skin around the site (C). Scale bars: 1 cm.

### Histological examination

The grafts were then examined histologically. Although the basic structure of the skin, that is, the epidermis and dermis, was reconstituted, every grafted site on the PGA(-) sponges contained epidermal cysts within the dermis and ectopic hair formation under the skin (Fig. 4B and Fig. 5A and B). Even when the hair sprouted out of the skin, the array was slightly disheveled. In some cases, many epidermal cysts were formed ( $9.6 \pm 3.2$  cysts/section), inasmuch that normal hair formation was completely disturbed (Fig. 5C and D).

In the case of the PGA(+) sponge, few epidermis cysts were observed ( $1.4 \pm 1.1$  cysts/section), and ectopic hair formation was far less than on PGA(-) sponge (Fig. 4B and Fig. 5E and G). Furthermore, on the PGA(+) sponge, the hair array was arranged regularly, sloping from head to tail. Sebaceous glands were normally generated.

The PGA(+) collagen sponge as a scaffolding did not seem to interfere with normal hair formation and outgrowth in the hair reconstitution assay.

### DISCUSSION

In the current study, we attempted to make the hair reconstitution assay more convenient and precise, by using a collagen sponge as a scaffold. Because collagen, the main component of the extracellular matrix, has superior cell affinity than other, synthetic molecules, it has been commonly used as a scaffold in three-dimensional skin reconstitution cultures, in which the construction of a structure suggestive of normal skin is generated *in vitro*.<sup>16-19</sup> In a three-dimensional skin culture using collagen sponges, a multilayered skin structure can be reconstituted. However, current three-dimensional reconstituted skin has no skin appendages, including hair

follicles and sweat/sebaceous glands. Thus, the influence of collagen sponges on the formation of skin appendages has not been investigated. Using a collagen sponge as a scaffold in this hair reconstitution assay, the method became more convenient and we could obtain highly reproducible results, that is, the rate of fixation and the appearance of every grafted site, compared with established methods, and we could perform quantitative evaluations such as hair density analysis. Such results suggest that the sponge could retain the grafted cells within itself and prevent the cell suspension from tilting and leaking out of the chamber. However, our study demonstrated that the conventional collagen sponge disturbed normal hair reconstitution. Therefore, we prepared a novel collagen sponge reinforced by PGA fiber, and this study suggests that normal hair growth can be seen at the grafted sites of the PGA(+) sponge, as compared with the conventional PGA(-) sponges.

Our results showed that epidermal cysts and ectopic hairs frequently formed on the conventional PGA(-) collagen sponge. One possible reason is that the volume of the PGA(-) sponge decreased as a result of humidity after the seeding of cell suspension, because collagen was weaker. Thus, because the pore structure size of the sponge shrank, the deflated collagen sponge might inhibit the movement of the transferred cells, with epidermal cysts consequently forming in the grafted sites. Moreover, the shrinkage of PGA(-) sponges might also result in the leakage of cell suspension that could not be retained within the collagen sponge. Therefore, it might cause enlargement of the grafted sites and ectopic hair formation. Thus, with use of the conventional sponge alone, the proper reconstitution of hair follicles cannot be fully achieved.

The synthetic polymers PGA and poly-L-lactic acid (PLLA) have been commonly used in clinical fields. The time over which PGA biodegrades (approximately 1

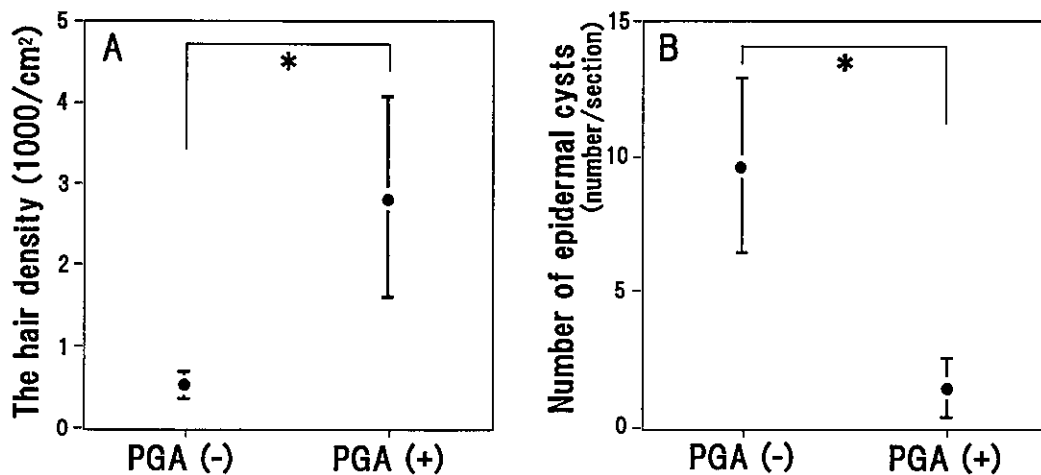
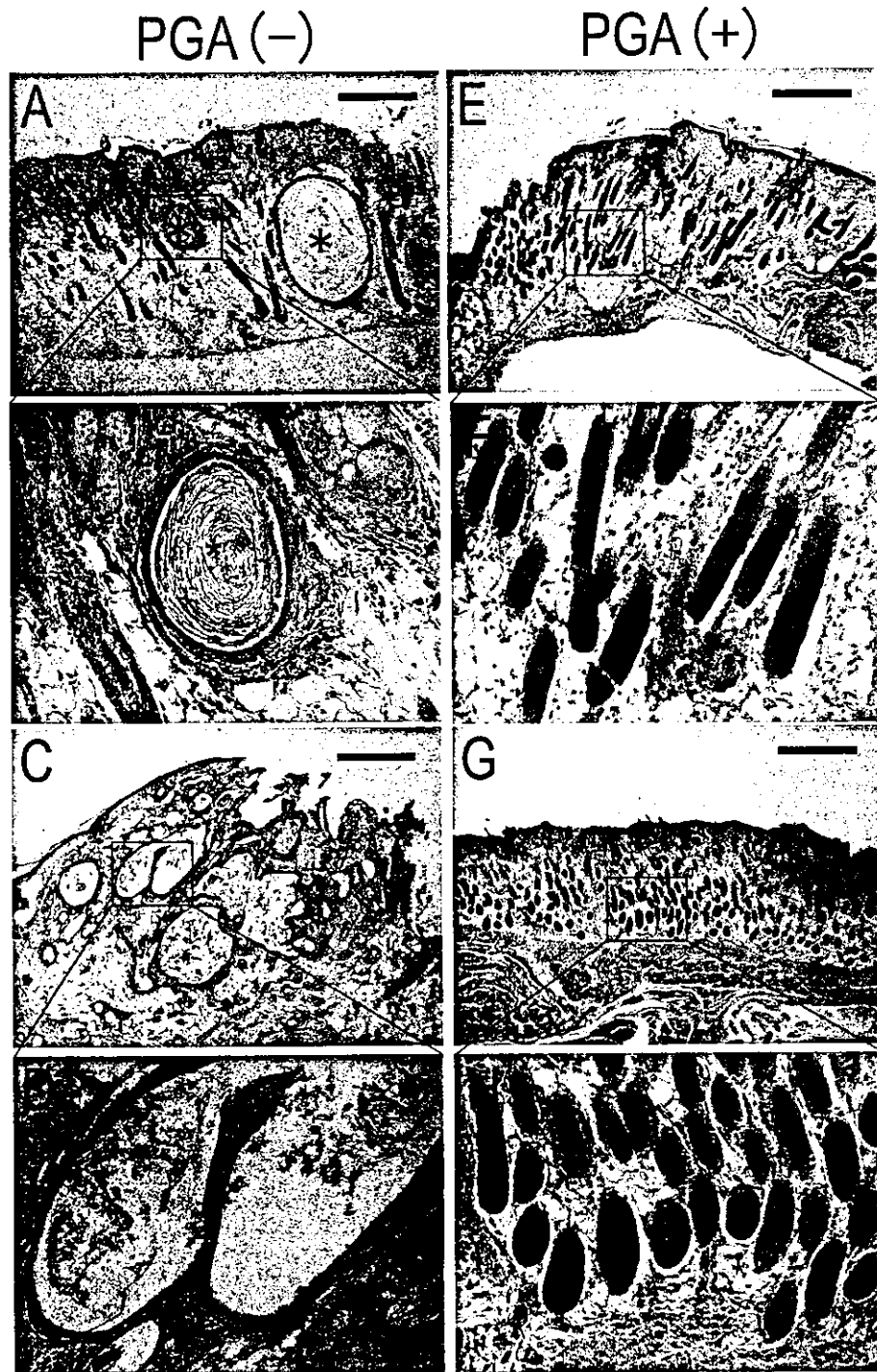


FIG 4. Hair density (A) and number of epidermal cysts (B) on the grafted site. \* $p < 0.05$ .



**FIG 5.** Microscopic appearance of the grafted sites on PGA(-) sponge (A-D) and PGA(+) sponge (E-H). On PGA(-) sponge, epidermal cyst formation (A and B, asterisk) and disturbed hair formation (C and D) were frequently observed. (E-H) Hair array was arranged regularly on PGA(+) sponge. Scale bars: 500  $\mu$ m. Original magnification: (A, C, E, and G)  $\times 40$ ; (B, D, F, and H)  $\times 200$ . H&E staining.

month) is much shorter than that of PLLA, (approximately 2 years). Moreover, the biocompatibility of PGA is better than that of PLLA, but neither is as good as collagen.<sup>14</sup> We then created a novel scaffold, which has the

advantageous properties of both collagen and synthetic polymer, using PGA fiber. Because the incorporation of PGA fibers mechanically reinforces the collagen sponge, the PGA(+) sponge had less shrinkage, thereby maintain-